Pressure and temperature dependence of the structure of liquid InSb

T. Hattori, T. Kinoshita, N. Taga, Y. Takasugi, T. Mori, and K. Tsuji
Department of Physics, Keio University, Yokohama 223-8522, Japan
(Received 20 October 2004; revised manuscript received 13 May 2005; published 12 August 2005)

We investigate the structure of liquid InSb over a wide pressure range up to 20 GPa and a wide temperature range up to 1570 K by synchrotron x-ray diffraction. With increasing pressure along the melting curve, the local structure, which is anisotropic near the ambient pressure, becomes more isotropic. However, at pressures higher than about 10 GPa, the pressure-induced change becomes less prominent, and the local structure contracts almost uniformly. Structural parameters deviate significantly from those in simple liquid metals in this pressure region, revealing a stable liquid form with an anisotropic local structure. The analysis of $g(r)$ reveals that the liquid is possibly interpreted by the local structure of a *single species*, whose $g(r)$ is apparently expressed by a linear combination of $g(r)$ for β-Sn-like and bcc-like local structures in a one-to-one ratio. This local structure is completely different from those present in its crystalline counterpart. Pressure and temperature dependence of the local structure is discussed in the relation to Rapoport two species model [J. Chem. Phys. **46**, 2891 (1967)].

DOI: 10.1103/PhysRevB.72.064205 PACS number(s): 61.20.Qg, 62.50.+p, 61.10.Eq, 07.35.+k

I. INTRODUCTION

Pressure- and temperature-induced changes in structures and physical properties of materials are of fundamental interest in condensed matter physics. In spite of this, changes in liquid matter have not been investigated as much as those in crystalline matter, due to limited structural information and experimental difficulties. It is interesting to reveal the pressure and temperature dependence of liquid structure, because liquid phases would likely display marked differences from crystalline phases due to differences in the fluctuations of structural parameters such as bond length and bond angles.

Among several liquids, tetrahedrally bonded materials, such as liquids of group 14 elements and liquid III-V compounds, attract a great deal of attention because of their pressure-induced evolution in chemical bonding (from a covalent type to a metallic one[1]) and because of the possible existence of a first-order liquid-liquid phase transition.[2–4] At ambient pressure, these liquids are known to have the following characteristics.[5,6]

(i) The structure factor $S(Q)$ has a hump on the high-Q side of the first peak. This indicates the existence of a specific angular correlation between interatomic bonds. From this fact, we can find that the structure of the liquids cannot be interpreted by the particle having an isotropic potential. Hereafter, we describe such local structure as anisotropic.

(ii) The height of the first peak in $S(Q)$, $S(Q_1)$ is much smaller than that in simple liquid metals.

(iii) The ratio of the wave numbers between the first and second peaks in $S(Q)$, Q_2/Q_1, which is related to anisotropy in a local structure, is much larger than that in simple liquid metals.[7]

(iv) The trough between the first and the second peaks in the pair distribution function $g(r)$ is much shallower than that in simple liquid metals.

(v) The coordination number CN is much smaller (≈ 6) than that for simple liquid metals [10–11 (Ref. 7)].

These features indicate that liquids of tetrahedrally bonded materials have anisotropic local structures. In spite of past efforts, their local structures are still unidentified. As a candidate, a local structure similar to the crystal structure of a high-pressure crystalline phase (β-Sn structure) having partial covalent bonding is proposed.[8,9] The existence of the covalent bonds in the liquids is supported by first-principle molecular dynamics simulations.[1,10] These facts imply that the covalent nature of their chemical bonds is preserved, even after metallization on melting. Because of the covalent bonds, contraction and expansion behaviors of the liquids of tetrahedrally bonded materials are different from those in simple liquid metals.[1,4,11–13] The main purpose of the present study is to reveal the pressure and temperature dependence of the structure of these materials. Continuing our previous studies on liquids of group IV elements[4,11,12,14] and liquid GaSb (l-GaSb),[13] we investigate the liquid structure of InSb, which has a larger ionic character than the previous materials.

The PT phase diagram of InSb is shown in Fig. 1, together with the experimental conditions of the present study. Despite extensive research on the subject (Ref. 15 and references therein), the phase diagram is still the subject of debate. The central problem is the difficulty in determining *thermodynamically* stable phases due to the sluggish transformation as well as the complex structures of the high-pressure phases. In the high temperature region, however, the difficulty is mitigated by the decreasing transformation kinetics. With increasing pressure along the melting curve, the crystal structure changes from the zinc-blende structure to the orthorhombic *Immm* structure, and finally to the bcc structure. Noticeably, in the high temperature region, the bcc structure appears at a pressure much lower than that reported previously in room-temperature experiments.[16,17]

II. EXPERIMENT

Experiments were performed by an energy-dispersive x-ray diffraction method (EDX) using a synchrotron-

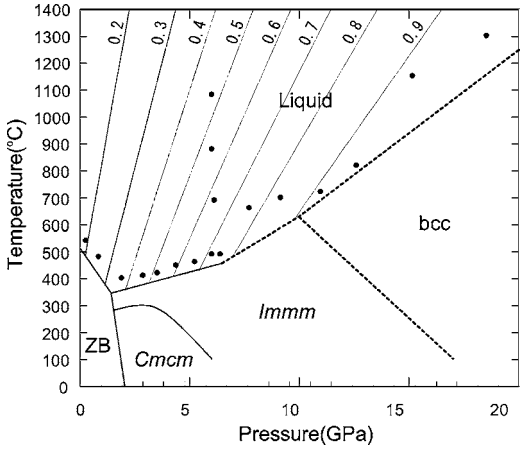

FIG. 1. The phase diagram of InSb and the experimental PT conditions in this study. The phase boundaries shown by solid lines are after Ref. 15 and references therein. Those shown by dotted lines are determined in this study. The isofraction lines of the denser form, y, are also presented (see Sec. IV D).

radiation source. Two types of multianvil high-pressure apparatuses were used for compression. For data collection below 13.2 GPa, we used the single-stage high-pressure apparatus, MAX80, installed at AR-NE5C in the High Energy Accelerator Research Organization (PF-AR, KEK). For data collection above 15.9 GPa, we used the Kawai-type double-stage high-pressure apparatus, SPEED1500, installed at BL04B1 in the SPring-8.[18] The diffraction intensity was collected with a pure Ge solid-state detector. Reagent-graded InSb with a purity of 99.999% (Rare Metallic Co., Ltd.) was used as the sample. To avoid too much x-ray absorption, we mixed NaCl with the sample so that μt becomes equal to 2 for x-ray energy $E=40$ keV. Here, μ is an average linear absorption coefficient and t is the thickness of the sample. The cell assemblies used in the high-pressure experiments were almost the same as those described in Refs. 19 and 20. Melting of the sample was judged from the appearance of a halo pattern, as well as the disappearance of all the Bragg peaks. The chemical composition of the sample was checked by measuring characteristic x-ray intensities for In and Sb. Deviation of the chemical composition of the sample from the initial one (InSb) was not observed during the experiment. We took diffraction profiles at various 2θ angles[21] to obtain $S(Q)$ over a wide Q range (at least up to $Q=15$ Å^{-1}).

To reveal the pressure and temperature dependence of the structure of l-InSb, we took data along two PT paths, (i) high-pressure conditions along the melting curve and (ii) high-temperature conditions at a constant pressure (6.3–6.4 GPa) (see Fig. 1). Pressure was determined from the lattice parameter of the pressure marker (NaCl) based on the equation of state.[22] Temperature was estimated from the electric power applied to the heater. The relation between temperature and electric power was determined beforehand. The accuracy of pressure and temperature was within 0.7 GPa and 100 K in the pressure region below 6 GPa, and 1.4 GPa and 200 K in the pressure region above 6 GPa.

The $S(Q)$ was deduced from the diffraction intensity taken at various 2θ angles. The $g(r)$ was obtained through the Fourier transformation of $S(Q)$. The $S(Q)$ and $g(r)$ in this study are based on the definition by Faber and Ziman.[23] The average number density of the liquid ρ_0 is estimated by the procedure described in Ref. 13. The error of the estimation is within 3% for the data at 50 K above the melting temperature. The structural information on l-InSb is summarized in Tables I and II.

III. RESULTS

A. Pressure dependence

The pressure dependence of $S(Q)$ is shown in Fig. 2(a). Near the ambient pressure (0.3 GPa), the local structure of liquid is found to be highly anisotropic. $S(Q)$ has a characteristic hump ($Q_h \approx 3$–3.5 Å^{-1}) on the high-Q side of the first peak. The height of the first peak is much smaller than that

TABLE I. Structural information of l-InSb at high pressures.

P (GPa)	Q_1 (Å^{-1})	Q_2 (Å^{-1})	Q_2/Q_1	$S(Q_1)$	$S(Q_2)$	r_1 (Å)	r_2 (Å)	r_2/r_1	CN
0.3(1)	2.21(1)	4.68(2)	2.11(1)	1.78	1.12	3.01(1)	6.44(2)	2.14(1)	5.6(4)
0.9(1)	2.23(1)	4.64(2)	2.08(1)	2.01	1.12	3.04(1)	6.34(2)	2.09(1)	6.4(4)
2.0(3)	2.25(1)	4.60(2)	2.04(1)	2.31	1.15	3.04(1)	6.23(2)	2.05(1)	6.4(4)
3.0(2)	2.27(1)	4.58(2)	2.02(1)	2.35	1.16	3.03(1)	6.17(2)	2.04(1)	6.7(4)
3.7(1)	2.29(1)	4.59(2)	1.99(1)	2.48	1.17	3.04(1)	6.12(2)	2.01(2)	6.9(4)
4.6(2)	2.30(1)	4.59(2)	1.99(1)	2.53	1.18	3.02(1)	6.08(2)	2.01(1)	7.1(4)
5.5(2)	2.32(1)	4.60(2)	1.99(1)	2.49	1.16	3.00(1)	6.05(2)	2.02(1)	6.7(4)
6.7(1)	2.33(1)	4.62(2)	1.98(1)	2.56	1.18	3.01(1)	6.00(2)	2.00(1)	7.1(4)
8.1(1)	2.34(1)	4.57(2)	1.95(1)	2.55	1.19	3.03(1)	5.98(2)	1.98(1)	7.2(4)
9.6(2)	2.36(1)	4.60(2)	1.95(1)	2.65	1.17	3.02(1)	5.95(2)	1.97(1)	7.5(4)
11.5(1)	2.38(1)	4.60(2)	1.93(1)	2.58	1.17	3.01(1)	5.91(2)	1.96(1)	7.5(4)
13.2(1)	2.40(1)	4.63(2)	1.93(1)	2.73	1.17	2.99(1)	5.86(2)	1.96(1)	7.3(4)
15.9(3)	2.42(1)	4.67(2)	1.93(1)	2.61	1.15	2.96(1)	5.79(2)	1.96(1)	8.3(4)
19.4(2)	2.45(1)	4.72(2)	1.93(1)	2.66	1.15	2.93(1)	5.71(2)	1.95(1)	7.7(4)

TABLE II. Structural information of *l*-InSb at high temperatures at constant pressure (P=6.3–6.4 GPa).

T (K)	Q_1 (Å^{-1})	Q_2 (Å^{-1})	Q_2/Q_1	$S(Q_1)$	$S(Q_2)$	r_1 (Å)	r_2 (Å)	r_2/r_1	CN
760	2.33(1)	4.58(2)	1.96(1)	2.64	1.19	3.02(1)	6.03(2)	2.00(1)	7.3(4)
960	2.33(1)	4.62(2)	1.99(1)	2.30	1.15	3.00(1)	6.05(2)	2.02(1)	6.5(4)
1150	2.32(1)	4.68(2)	2.02(1)	2.13	1.13	2.98(1)	6.07(2)	2.04(1)	6.3(4)
1350	2.32(1)	4.71(2)	2.04(1)	2.06	1.13	2.98(1)	6.06(2)	2.04(1)	6.3(4)
750									7.1(2)[a]

[a]Estimated from the pressure dependence of CN.

for simple liquid metals [≈2.5–3.0 (Ref. 7)]. The ratio of the wave numbers between the first and the second peaks, Q_2/Q_1, which is related to the anisotropy of the local structure, is much larger than the value typical for simple liquid metals [≈1.86 (Ref. 7)]. These features are commonly observed in $S(Q)$ of liquid group IV elements and liquid III-V compounds at ambient pressure.[8,24] By compression, the anisotropy of the local structure decreases. The hump becomes smaller and the first peak becomes higher. The Q_2/Q_1 ratio becomes smaller (Fig. 3) due to a shift of the first peak toward a high Q value and a less significant shift of the second peak. These features suggest that *l*-InSb contracts nonuniformly. By further compression, pressure-induced changes become less prominent. For example, the Q_2/Q_1 ratio does not change markedly in the high-pressure region ($P > \approx 10$ GPa) (Fig. 3). The height of the peaks and the hump remain unchanged. This suggests that *l*-InSb contracts almost uniformly in the high-pressure region. This also implies the existence of a relatively stable liquid form which is not changed by compression in the high-pressure region ($P > \approx 10$ GPa). Noticeably, in that region, the structural parameters deviate from those of simple liquid metals: the hump remains and the Q_2/Q_1 ratio is much larger than that for simple liquid metals. This indicates that the stable liquid form has anisotropy in the local structure. Surprisingly, the liquid contracts *uniformly* despite the *anisotropy* of the local structure.

The pressure dependence of $g(r)$ is shown in Fig. 2(b). Near ambient pressure (0.3 GPa), the $g(r)$ has a hump on the large r side of the first peak ($r \approx 4.1$ Å). The trough between the first and second peaks is relatively shallow compared to that for simple liquid metals. The ratio of the positions between the first and the second peaks, r_2/r_1 (≈2.14 at 0.3 GPa), is much larger than that for simple liquid metals [≈1.84–1.90 (Ref. 7)]. These features are consistent with results reported previously.[25] By compression, the second and third peaks shift toward smaller r values, which is obvious in the pressure dependence of the peak positions normalized by the respective values at ambient pressure (Fig. 4[26]). Simultaneously, the height of the second and third peaks increases and the hump becomes less prominent. The trough between the first and the second peaks becomes deeper. These features indicate that the local structure of the liquid becomes simpler with increasing pressure. In spite of significant change in the positions of the second and the third peaks, the first peak does not shift markedly in the low pressure region ($P < \approx 10$ GPa) (Fig. 4). This fact indicates that the nearest-neighbor distance does not change markedly in this pressure region. By further compression, all of the peaks shift toward small r values at the same rate (Fig. 4). The

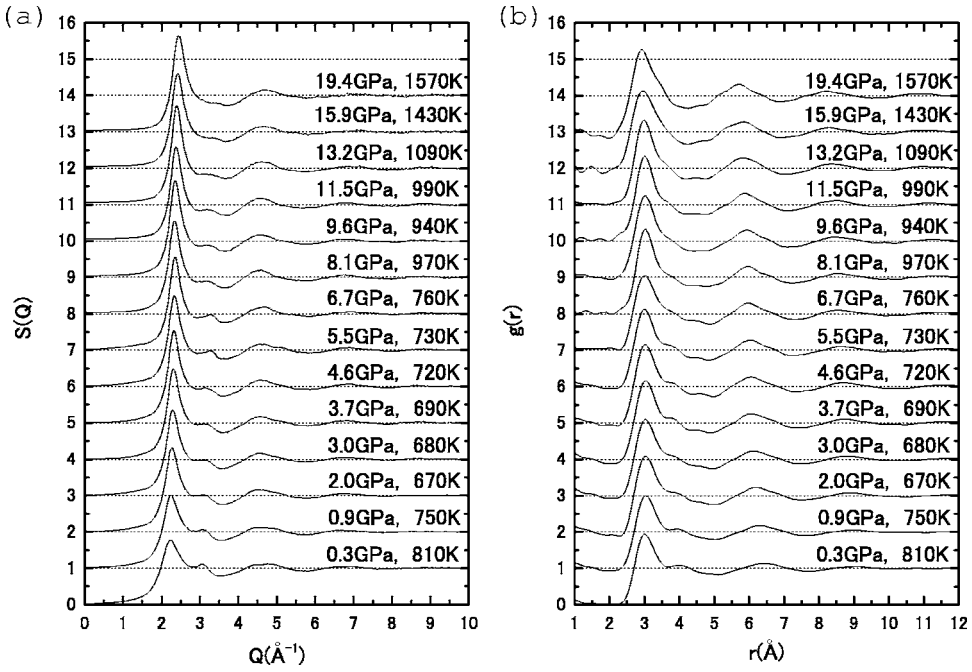

FIG. 2. (a) The $S(Q)$ of *l*-InSb at high pressures. Here, we present profiles only up to $Q = 10$ Å^{-1} to show the pressure dependence more clearly. (b) The $g(r)$ of *l*-InSb at high pressures. We use the $S(Q)$ in the Q region up to 13.8 Å^{-1} to deduce the $g(r)$.

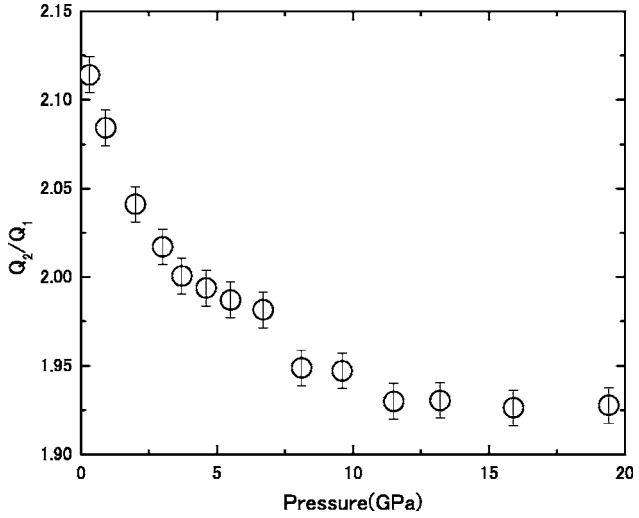

FIG. 3. Pressure dependence of Q_2/Q_1 in *l*-InSb.

change in the shape of the profile for $g(r)$ is no longer observed in the high pressure region ($P > \approx 10$ GPa). These features indicate that *l*-InSb contracts almost uniformly in this pressure region. The above-mentioned high-pressure behavior in $g(r)$ is consistent with that in $S(Q)$.

To reveal the change in the local structure, we deduce CN from a radial distribution function RDF [$=4\pi r^2\rho_0 g(r)$]. In binary liquids, four partial coordination numbers, $CN_{A\text{-}A}$, $CN_{A\text{-}B}$, $CN_{B\text{-}A}$, $CN_{B\text{-}B}$, are defined. Here each $CN_{I\text{-}J}$ represents the number of J-type atoms around an I-type atom. In the present study using the EDX method, we cannot obtain these numbers because we cannot obtain partial pair-distribution functions, $g_{In\text{-}In}$, $g_{In\text{-}Sb}$, and $g_{Sb\text{-}Sb}$. Therefore, we estimate the average CN for two states with different chemical short-range orders, i.e., a completely ordered state and a completely disordered one. In the case of InSb, the CN deduced for both states, however, become effectively the same (the difference is within 0.04%) because of the small difference of the atomic scattering factors between In and Sb.

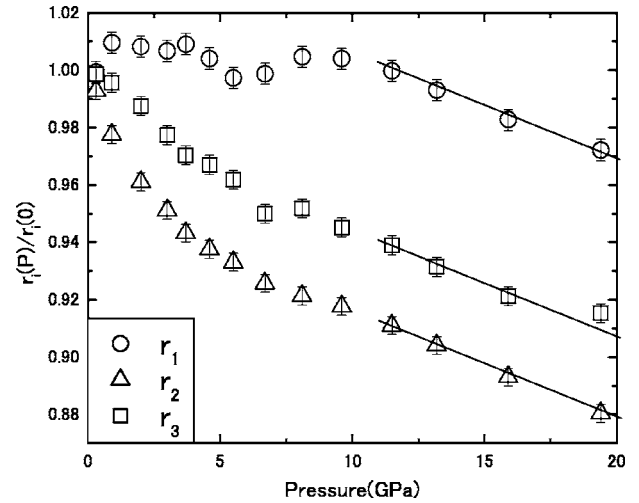

FIG. 4. Pressure dependence of positions of the peaks in $g(r)$. Each value is normalized by the respective one at ambient pressure. Solid lines are only guides for the eye.

Therefore, the CN deduced for the complete ordered model is shown in Table I (and also in Table II). The details of the calculation procedure is described in Ref. 13. The average CN is deduced on the basis of the following equation:

$$\mathrm{CN} = 2\int_{r_0}^{r_{\max}} 4\pi r^2 \rho_0 g_{\mathrm{total}}(r)\,dr. \tag{1}$$

Here, $g_{\mathrm{total}}(r)$ is the total $g(r)$ in the Faber-Ziman definition.[23] The r_0 is the low-r limit of the first peak in RDF, and $r_{\max}$ is the r value at the top of the first peak in RDF.

Near ambient pressure (0.3 GPa), CN ($\approx$5.6) is much smaller than the value typical for simple liquid metals [10–11 (Ref. 7)]. With compression, the CN markedly increases. By further compression ($P > \approx 10$ GPa), the rate of increase in CN becomes smaller and the CN approaches 8 ± 1. The saturation of the increase in the high pressure region implies that the change of the local structure finishes and the liquid takes a stable high-pressure form. Noticeably, the CN in this region is still much smaller than the value typical for simple liquid metals (10–11). It implies that the local structure in the high pressure region is still much different from that for simple liquid metals.

B. Temperature dependence

The temperature dependence of $S(Q)$ at the constant pressure of $P = 6.3$–6.4 GPa is shown in Fig. 5(a). This pressure is in the range where the liquid structure changes sensitively by compression. With increasing temperature, the position of the first peak shifts toward a smaller Q value, while those of the second and the third peaks shift toward large Q values (Table II). Consequently, the Q_2/Q_1 ratio increases (Table II). The temperature-induced deviation of Q_2/Q_1 from that of simple liquid metals [$\approx$1.86 (Ref. 7)] implies that the local structure becomes more *anisotropic* with increasing temperature. This view is also supported by the relative increase of the height of the hump at 3–3.5 Å^{-1}, the height of the hump is constant (or slightly increases) while those for the other peaks become smaller due to the temperature-induced increase in structural fluctuation. The hump is observed at 1350 K, which suggests that the anisotropic local structure in the liquid is preserved at a temperature much higher than the melting point.

The temperature dependence of $g(r)$ is shown in Fig. 5(b). As the temperature is raised, the first peak shifts toward a small r value in spite of heating, while the second and third peaks normally shift toward a large r value. Consequently, the r_2/r_1 ratio becomes larger with increasing temperature (Table II). Simultaneously, the height of the hump on the large r side of the first peak remains constant, although the amplitude of the oscillation in $g(r)$ becomes smaller. These results also support the view suggested from the temperature dependence of $S(Q)$.

The CN at high temperatures are shown in Table II. The CN decreases with increasing temperature. This behavior can be explained by the following two mechanisms. The first is the formation of voids in the liquid structure (hereafter we call this "the void-increase model"). The other is a change in

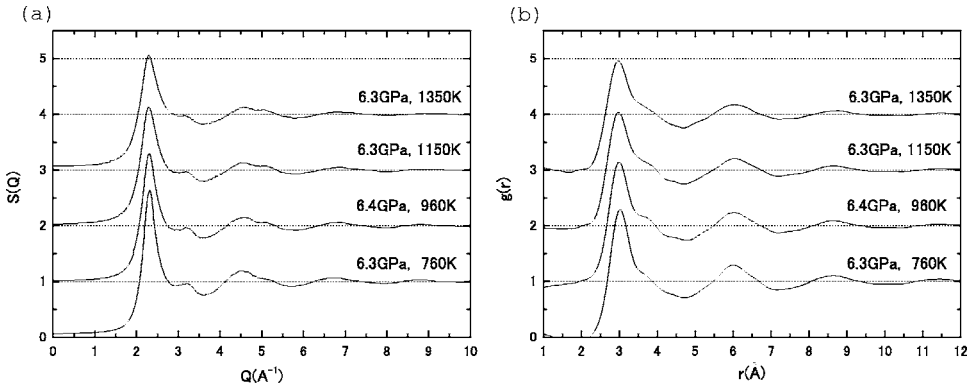

FIG. 5. (a) The $S(Q)$ of l-InSb at high temperatures. Here, we present profiles only up to $Q = 10$ Å^{-1} to show the pressure dependence more clearly. (b) The $g(r)$ of l-InSb at high temperatures. We use the $S(Q)$ in the Q region up to 13.8 Å^{-1} to deduce $g(r)$.

the local structure from a highly coordinated form into a less-coordinated one. The latter mechanism is found to occur in l-InSb from the comparison of the temperature dependence of CN with that expected from the void increase model (Sec. IV B) and from results of local structure analysis (Sec. IV C).

IV. DISCUSSION

A. Pressure dependence

1. Comparison with simple liquid metals

The contraction behavior of simple liquid metals has previously been investigated.[27,28] The following features were reported.

(i) The $S(Q)$ and $g(r)$ monotonically shift toward a larger Q value and a smaller r value, respectively, without significant changes in the shapes of the profiles.

(ii) The structural parameters, such as Q_2/Q_1, r_2/r_1, and CN, remain unchanged in spite of compression.

These features can be explained by the uniform contraction model. In this model, the liquid contracts by decreasing the nearest-neighbor distance rather than by changing its CN. The above-mentioned features are completely different from those observed in l-InSb in a low pressure region. The pressure dependence of $S(Q)$, $g(r)$, and CN implies that l-InSb contracts by changing its local structure from a low-coordinated form into a highly coordinated one, rather than by shrinking the local structure itself. This view is also supported by the results of the local-structure analysis in Sec. IV C.

In contrast, the contraction behavior observed in the high-pressure region is almost the same as that for simple liquid metals. In this pressure region, l-InSb contracts mainly by shrinking the local structure isotropically while maintaining the same CN. This view is supported by the pressure-induced decrease in r_1 and the lack of detectable change in CN at high pressures. Also, the lack of significant change in the local structure is supported by the results of the local structure analysis in Sec. IV C.

2. Comparison with other tetrahedrally bonded materials

The contraction behaviors of the liquids of tetrahedrally bonded materials, such as liquid Si (l-Si), liquid Ge (l-Ge), l-GaSb, and liquid InAs (l-InAs), have previously been investigated.[1,4,11,13,29] All these liquids show the following features.

(i) The shapes of the profiles of $S(Q)$ and $g(r)$ significantly change with increasing pressure. For example, the first peak in $S(Q)$ becomes higher. The hump on the high Q side of the first peak becomes smaller. The second and third peaks in $g(r)$ become higher. The trough between the first and second peaks in $g(r)$ becomes deeper.

(ii) The Q_2/Q_1 and r_2/r_1 ratios become smaller with increasing pressure and they approach their respective values for simple liquid metals.

(iii) The CN gradually increases by compression.

The l-InSb also shows these features in a low-pressure region ($P < \approx 10$ GPa). This indicates that l-InSb contracts in the same way as the liquids of other tetrahedrally bonded materials in this region.

To compare the contraction behavior more quantitatively, the pressure dependence of the Q_2/Q_1 ratio for l-InSb is shown together with those for l-Si, l-Ge, l-GaSb, and l-InAs (Fig. 6). Near ambient pressure, l-InSb has a value similar to those for the other liquids. Roughly speaking, the ratio of l-InSb decreases in the same manner as those of the other liquids with increasing pressure. The value for l-InSb decreases at a higher rate than any other liquid. Consequently, l-InSb has the smallest value at pressures below 10 GPa. This behavior is explainable by the empirical rule widely known in crystalline phases, heavy elements show the high-pressure states of the lighter elements at the lower pressure. The comparison of the pressure dependence of the liquids implies that the empirical rule is also valid for liquid states. On the basis of this rule, from the pressure depen-

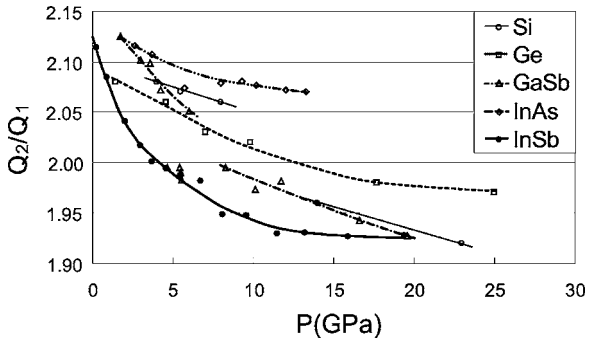

FIG. 6. Comparison of the pressure dependence of Q_2/Q_1 in several liquids. The data are taken from Refs. 11, 13, 20, and 29.

dence in *l*-InSb we are able to anticipate the high-pressure behavior for the other liquids in the pressure region where investigations have not been done. As observed in *l*-InSb, the liquids of other tetrahedrally bonded materials would change their contraction behavior from a nonuniform type into a uniform one around the pressure where the Q_2/Q_1 ratio becomes 1.93. In the higher pressure region, the relatively stable local structure with anisotropy would appear in the liquids. In the past, it was believed from the successive decrease in the Q_2/Q_1 ratio that liquids of tetrahedrally bonded materials monotonically approach simple liquid metals at high pressures. The results of the present study belie this view and suggest the new view that the liquids approach the nonsimple liquid with the Q_2/Q_1 ratio of ≈ 1.93. This view is also supported by our results on liquid Sn (*l*-Sn), in which the Q_2/Q_1 ratio is about 1.93 over a wide pressure range from 3 GPa to 20 GPa.[14]

B. Temperature dependence

1. Comparison with simple liquid metals

Temperature dependence of the structure of simple liquid metals has previously been investigated.[30,31] The following features are reported:

(i) The position of the first peaks in $S(Q)$ and $g(r)$ does not change.

(ii) The height of the first peaks in $S(Q)$ and $g(r)$ decreases with increasing temperature.

(iii) The CN decreases proportionally to number density.

These features are explainable by the void-increase model. On the other hand, those observed in *l*-InSb are very different from these. For example, the position of the first peak in $g(r)$ significantly decreases and the Q_2/Q_1 and r_2/r_1 ratios increase with increasing temperature. To confirm that the high-temperature behavior of *l*-InSb cannot be explained by the void increase model, we compare the temperature dependence of CN with that expected for the void increase model (Fig. 7). In the figure, the number density normalized by the value at 760 K (50 K above the melting temperature) at 6.3 GPa is also shown. With increasing temperature (with decreasing number density), the CN decreases at the rate larger than that expected for the void-increase model. This fact clearly shows that the high-temperature behavior of *l* -InSb is not explainable by the void increase model. This also suggests that *l*-InSb expands through a change in the local structure from a highly coordinated form into a less-coordinated one at high temperatures.

2. Comparison with other tetrahedrally bonded materials

Temperature dependence of the structure have previously been investigated in *l*-Si, *l*-Ge, *l*-Sn, *l*-GaSb, and *l*-InSb.[9,24,25,32,33] These liquids show almost the same high-temperature behaviors. The characteristic features are shown below.

(i) The hump on the high-Q side of the first peak in $S(Q)$ is preserved at temperatures much higher than the melting point T_m. For example, the hump is preserved at T_m +110 K for *l*-Si, T_m+250 K for *l*-Ge, T_m+1370 K for *l*-Sn, and T_m+338 K for *l*-GaSb. This indicates that these liquids preserve anisotropic local structures at temperatures much higher than their melting points.

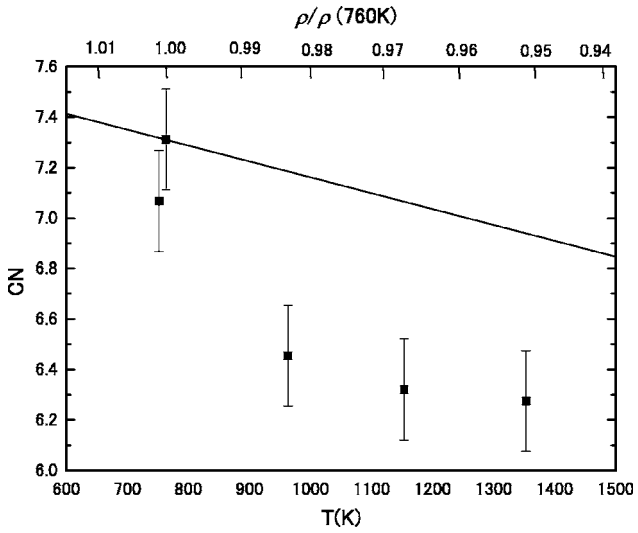

FIG. 7. The CN of *l*-InSb at high temperatures. The CN at 6.3 GPa, which is estimated from the pressure dependence of CN, is also shown. The temperature dependence expected for the void-increase model is shown by a solid line.

(ii) Roughly speaking, the shape of the profile in $S(Q)$ and $g(r)$ does not change except for smearing of the oscillation of the profiles.

The lack of significant change in the local structure would be caused by the fact that the temperature range of the investigation is too limited to observe the change. On the other hand, slight but significant changes were reported in *l*-Sn.[33] The following features were reported in addition to the aforementioned characteristics.

(iii) The Q_2/Q_1 ratio increases as the temperature is raised.

(iv) The CN decreases with increasing temperature.

These features are also observed in this study (see Sec. III B). From the similarity, the *l*-InSb is considered to expand by the same mechanism as that for *l*-Sn. Since *l*-Sn liquid is known to preserve the fragment of the tetrahedral local structures at temperatures much higher than its melting point,[33] *l*-InSb is also considered to preserve the anisotropic local structure at temperatures much higher than its melting point.

C. Analysis of the local structure

1. Analysis based on two species of the β-Sn-like and bcc-like local structures

To estimate the local structure in *l*-InSb, we compare the experimental $g(r)$ with those simulated using a simple model. The model consists of a distorted-crystalline model and a two species model (TSM). The detailed procedure is shown in Ref. 13. In our previous study on *l*-GaSb,[13] we found that the model successfully reproduces the experimental $g(r)$. In this study, we also find that the model successfully reproduces the experimental $g(r)$ of *l*-InSb as shown later. However, the validity of the model is not yet estab-

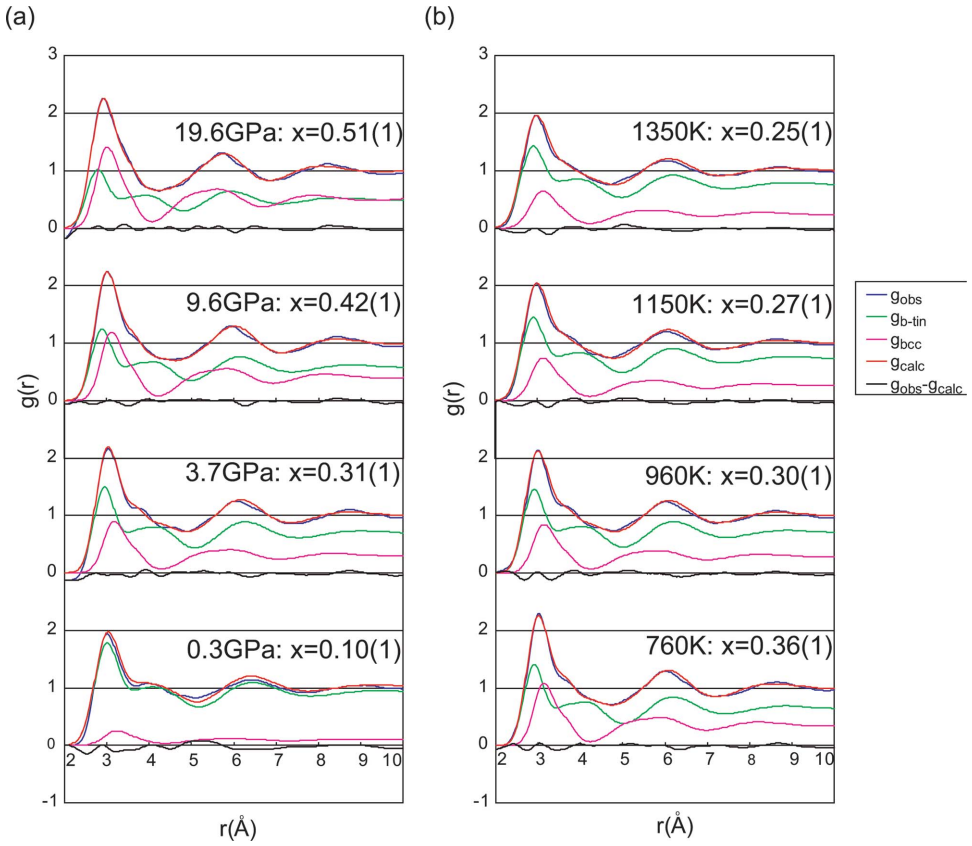

FIG. 8. Typical results of the fitting of the experimental $g(r)$ by a set of the models (the distorted-crystal model and two species model). The x means the fraction of the bcc-like form. The simulated $g(r)$ is constructed by a linear combination of $g(r)$ for β-Sn-like and bcc-like local structures. The $g(r)$ for each structure is weighted by the fractional ratio. The difference between the experimental and simulated $g(r)$ is shown together. (a) Pressure dependence. (b) Temperature dependence at a constant pressure (P = 6.3–6.4 GPa).

lished, so the results of this analysis provide a possible model for the local structure of l-InSb. Further investigation should be carried out by using another method, such as a molecular-dynamic simulation.

Here, we briefly mention the simulation procedure. First, we simulate $g(r)$ for liquid from crystal structures by giving the Gaussian-type bond distribution. Then, these are combined taking it into consideration that the liquid may consist of two species with different densities. In the simulation, we introduce the following parameters: the specific volume of the local structure V/Z, the distribution of the nearest-neighbor distance σ_1, the degree of the loss of short-range order at a larger interatomic distance t, the fraction of a high-pressure form x. Here, we assume that V/Z, σ_1, and t are the same for both species. Thus, the number of all the free parameters becomes four. We optimize these parameters so that the difference between the observed and the calculated $g(r)$ is minimized. We test various pairs of the crystal structures previously reported in tetrahedrally bonded materials and their high-pressure phases, such as zinc-blende structure, orthorhombic *Cmcm* and *Immm* structures, bcc structure, β-Sn structure and body-centered-tetragonal (bct) structure.[34,35] When we use the pair of the β-Sn and bcc structures,[36] we obtain the best agreement [the average difference in $g(r)$ is within 5%]. Typical results of the fitting are shown in Fig. 8. The $g(r)$ is well reproduced by a linear combination of $g(r)$ for the β-Sn-like and bcc-like local structures. In spite of the successful fitting using this pair, these local structures are found to be inappropriate as the two species. In order to illustrate this, we first explain the high-pressure and temperature behavior of l-InSb using this pair. The pressure and temperature dependence of the fraction of the denser form (bcc-like local structure), x, is shown in Table III. As the pressure is raised, x gradually increases. However, the rate of increase becomes smaller and x stops increasing. To our surprise, half of the less dense form (β-Sn-like local structure) is preserved even at pressures where the bcc structure becomes more stable than β-Sn structure in the crystalline phases.[37] This behavior is unusual because most of the less dense form is likely to transform into the denser form. Actually, in the conventional Rapoport model,[38] such behavior is expected. In addition, the Rapoport model suggests the rate of the transformation is maximized around $x \approx 0.5$. The pressure dependence obtained in this analysis (Table III) contradicts this feature. Such a contradiction is also observed in the temperature dependence of x. With increasing temperature, the x decreases and approaches 0.25 (Table III). However, in Rapoport TSM, the fraction should approach 0.5 at high temperatures for reduction of the Gibbs free energy through the maximization of mixing entropy. Even if the fraction does not approach 0.5 for some reason, the x should increase by heating since the denser form with the bcc-like local structure would have an entropy larger than that for the β-Sn-like local structure.[39] The above-mentioned unusual behaviors require us to introduce other local structures as the two species of l-InSb.

2. Analysis based on the two species of the β-Sn-like structure and a new high-pressure one

The results on the pressure dependence of $S(Q)$, $g(r)$, and structural parameters imply the existence of a relatively stable local structure in the high-pressure region

TABLE III. Fraction of the denser form at high pressures and high temperatures, and the reliable factor of the fitting, R.[13]

P (GPa)	T(K)	Fraction,0 x [a]	R [b]
0.3(1)	810	0.10(1)	0.05
0.9(1)	750	0.18(1)	0.04
2.0(3)	670	0.24(1)	0.05
3.0(2)	680	0.27(1)	0.04
3.7(1)	690	0.31(1)	0.04
4.6(2)	720	0.31(1)	0.04
5.5(2)	730	0.30(1)	0.04
6.7(1)	760	0.32(1)	0.04
8.1(1)	970	0.39(1)	0.04
9.6(2)	940	0.42(1)	0.03
11.5(1)	990	0.44(1)	0.05
13.2(1)	1090	0.45(1)	0.04
15.9(3)	1430	0.48(1)	0.03
19.4(2)	1570	0.51(1)	0.03
6.3(1)	760	0.36(1)	0.03
6.4(1)	960	0.30(1)	0.04
6.3(2)	1150	0.27(1)	0.04
6.3(2)	1350	0.25(1)	0.04

[a]Fraction of the denser form (bcc-like local structure).
[b]The reliable factor is defined by the following equation: $R = \sqrt{(1/N)\Sigma_{i=0}^{N-1}[g_{\mathrm{obs}}(r_i) - g_{\mathrm{calc}}(r_i)]^2}$.

($P > \approx 10$ GPa). As shown in the preceding section, the $g(r)$ in this region is found to be well expressed by a linear combination of $g(r)$ for the β-Sn-like and bcc-like structures in the ratio of one to one. Hence, the single species apparently expressed by this combination is appropriate as the denser species of l-InSb, although the crystal structure corresponding to this form is not observed in crystalline-InSb (c-InSb). Hereafter we call this new form "0.5 β-Sn+0.5 bcc" for convenience. By introducing this form, we are able to explain the high-pressure and high-temperature behavior observed in this study. When we introduce the new form as the denser form instead of the bcc-like local structure, the fraction of the denser form is doubled. To avoid confusion, we denote the fraction of the new denser form as y. By introducing the new form, we find that the fraction of the denser form (0.5 β-Sn+0.5 bcc) increases from 0.0 to 1.0 as the pressure is raised. Moreover, the increasing rate becomes maximum around $y \approx 0.5$. These features are consistent with the Rapoport model. We are also able to explain the unusual behavior in temperature dependence. We find that the fractions of the low- and high-pressure forms approach 0.5 with increasing temperature. Our success in explaining the pressure and temperature dependence of the local structure by introducing the new form supports the validity of this local structure as the denser form. It is still unknown why this form (0.5 β-Sn +0.5 bcc) is stable. We hope it will be revealed by theoretical calculations.

3. Understanding of the pressure and temperature dependence in terms of the local structure change

We are able to understand the contraction behavior of l-InSb on the basis of the results of the local structure analysis. The l-InSb contracts nonuniformly in the low pressure region ($P < \approx 10$ GPa). In this pressure region, the fraction of the denser form increases significantly. Hence, the nonuniform contraction is considered to be caused by a change in the local structure from the β-Sn-like form into the denser form "0.5 β-Sn+0.5 bcc". In the high-pressure region ($P > \approx 10$ GPa), the liquid contracts almost uniformly. The results of the local structure analysis show that the transformation into the denser form is already completed at around 10 GPa. The almost uniform contraction is thus considered to be caused by the isotropic shrinking of the denser form.

The high-temperature behavior of l-InSb can also be explained by the temperature-induced change in the local structure. The temperature-induced increase of the anisotropy in the local structure is explainable by a change of the local structure from the denser form (0.5 β-Sn+0.5 bcc) into the less dense form (β-Sn-like local structure), since the latter form is considered to be more anisotropic. The decrease of CN at the larger rate than that expected from the void increase model is explainable by the same mechanism, since the less dense form has a smaller CN. A similar temperature behavior is observed in l-Sn. Itami *et al.*[33] reported that the Q_2/Q_1 ratio for l-Sn deviates more greatly from the value for simple liquid metals as the temperature is raised. Hosokawa *et al.*[40] also suggested that the covalent character in l-Sn becomes stronger at high temperatures. These facts imply that the fraction of an anisotropic local structure in l-Sn also increases with increasing temperature.

D. Application of the Rapoport two species model

To understand the pressure- and temperature-induced structural changes in l-InSb more quantitatively, we apply Rapoport model[38] to the fractions of two local structures. The detailed procedure is described in Ref. 13. In this model, the fraction of the denser form, y, is related to pressure and temperature by the following equation:

$$k_B T \ln\frac{y}{1-y} + (1-2y)w = \Delta\mu^0 (= \Delta\epsilon^0 - T\Delta S^0 + P\Delta V^0). \quad (2)$$

Here, k_B is the Boltzmann constant and w is the energy needed for the replacement of a like pair of local structures with an unlike pair. The parameters of $\Delta\mu^0$, $\Delta\epsilon^0$, ΔS^0, and ΔV^0 are, respectively, the differences in chemical potential, internal energy, entropy, and volume between the less dense and the denser forms. These parameters are assumed to be independent of pressure and temperature. The results of the fitting are shown in Fig. 9. Throughout the whole PT region of the present study the factions of the denser form are well reproduced by Rapoport model. The following parameters are determined in this analysis: $\Delta\epsilon^0 = -5.1 \times 10^{-22}$ (J/atom), $\Delta V^0 = 7.7$ (Å^3/atom), $\Delta S^0 = 3.6 \times 10^{-23}$ (J/K per atom), $\omega = -1.9 \times 10^{-20}$ (J/atom), and $\omega/k_B T$ (at $T = 1000$ K) $= -1.4$. The good reproducibility supports that the pressure and tem-

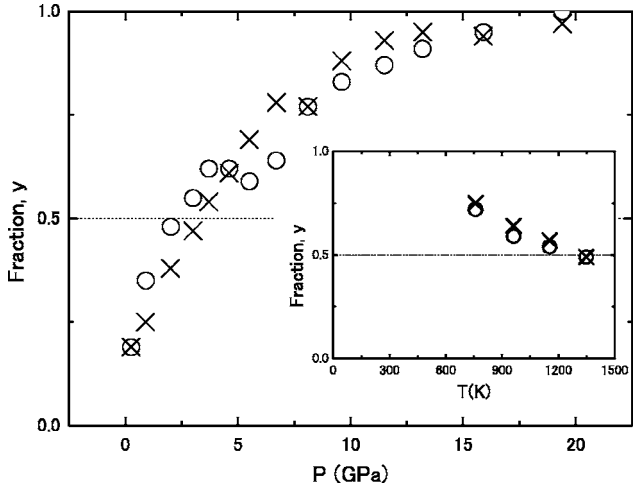

FIG. 9. Results of the fitting of the fraction of the denser form, y, by Rapoport model. Circle denotes the value calculated by the fitting of the experimental $g(r)$ with a set of the models (the distorted-crystal model and two species model). The cross denotes the value calculated with Rapoport model. The parameters used in the calculation are shown in the text.

perature dependence of the structure of l-InSb is well understood in terms of the change in the fraction of two local structures.

The iso-fraction lines for the denser form are estimated by the Rapoport model using the above parameters (Fig. 1). The iso-fraction lines are much inclined and are located over wide pressure range. The local structure, thus, gradually changes over wide pressure region. The same behavior is also observed in l-GaSb.[13,41] When we compare this with those reported for liquid Cs (l-Cs) and liquid Te (l-Te),[42] we find marked differences. In these liquids, the iso-fraction lines are steep and are located within a narrow pressure range. Consequently, the local structure changes drastically within a small pressure interval ($\Delta P < \approx 5$ GPa for l-Cs and $\Delta P < \approx 1.5$ GPa for l-Te). The different behavior is considered to originate from the fact that l-InSb and l-GaSb have the values w and ΔV^0 much smaller than those for l-Cs and l-Te, as is discussed in Ref. 13.

V. CONCLUSION

In order to reveal the pressure- and temperature-induced structural change in liquids of tetrahedrally bonded materials, we investigate the structure of l-InSb over a wide pressure and temperature range up to $\approx$20 GPa and $\approx$1570 K. The results are summarized as follows.

(i) The contraction behavior of l-InSb gradually changes from a nonuniform type into a uniform one. In a low-pressure region ($P < \approx 10$ GPa), the local structure becomes less anisotropic, while in the higher pressure region ($P > \approx 10$ GPa) the local structure contracts with maintaining its anisotropy. Significant deviation in structural parameters from those for simple liquid metals in the high-pressure region indicates the existence of the stable liquid form with an anisotropic local structure.

(ii) The l-InSb expands nonuniformly. As the temperature is raised, the anisotropy in the local structure increases. The CN decreases at a rate larger than that expected based on a void-increase model.

(iii) The l-InSb can be described by the mixture of two forms with different densities. The less dense form has a β-Sn-like local structure and the denser form has a local structure apparently expressed by a linear combination of β-Sn and bcc in the ratio of one to one. The latter structure is different from those realized in c-InSb.

(iv) The fraction of the denser form gradually increases with increasing pressure, whereas the increase becomes less prominent in the high pressure region. The nonuniform contraction observed in the low pressure region is attributed to a pressure-induced change in the local structure. The almost uniform contraction observed in the high pressure region is attributed to the isotropic shrink of local structures.

(v) As the temperature is raised at $P = 6.3$–6.4 GPa, the fractions of two forms approach 0.5. The nonuniform expansion of l-InSb is attributed to the change in the local structure from the dense form into the less dense one.

(vi) The pressure and temperature dependence of the structure of l-InSb is explainable by Rapoport two species model.

ACKNOWLEDGMENTS

The authors thank N. Funamori, T. Kikegawa, K. Funakoshi, and W. Utsumi for experimental support, and Y. Katayama, F. Shimojo, F. Yonezawa, H. Okumura, K. Nishio, and J. Kōga for valuable discussions. The authors thank D. Rockower for reading this paper. This work has been performed under the approval of the Photon Factory Program Advisory Committee (Proposal No. 2000G044) and of the Japan Synchrotron Radiation Research Institute (JASRI) (Proposal No. 2000B0037 and 2001B0472).

[1] J. Kōga, H. Okumura, K. Nishio, T. Yamaguchi, and F. Yonezawa, Phys. Rev. B **66**, 064211 (2002).
[2] P. H. Poole, T. Grande, C. A. Angell, and P. F. McMillan, Nature (London) **275**, 322 (1997).
[3] H. Tanaka, Phys. Rev. E **62**, 6968 (2000).
[4] N. Funamori and K. Tsuji, Phys. Rev. Lett. **88**, 255508 (2002).
[5] J. P. Gabathuler and S. Steeb, Z. Naturforsch. A **34A**, 1314 (1979).
[6] V. Petkov and G. Yunchov, J. Phys.: Condens. Matter **6**, 10885 (1994).
[7] Y. Waseda, *The Structure of Non-Crystalline Materials* (McGraw-Hill, New York, London, 1980).
[8] Y. Waseda and K. Suzuki, Z. Phys. B **20**, 339 (1975).
[9] V. Petkov, S. Takeda, Y. Waseda, and K. Sugiyama, J. Non-Cryst.

Solids **168**, 97 (1994).
[10] I. Stich, R. Car, and M. Parrinello, Phys. Rev. Lett. **63**, 2240 (1989).
[11] T. Mori, Master thesis, Keio University, 2000.
[12] K. Tsuji, T. Hattori, T. Mori, T. Kinoshita, T. Narushima, and N. Funamori, J. Phys.: Condens. Matter **16**, S989 (2004).
[13] T. Hattori, K. Tsuji, N. Taga, Y. Takasugi, and T. Mori, Phys. Rev. B **68**, 224106 (2003).
[14] T. Narushima, T. Hattori, T. Kinoshita, and K. Tsuji (unpublished).
[15] M. Mezouar, J. M. Besson, G. Syfosse, J. P. Itié, D. Häusermann, and M. Hanfland, Phys. Status Solidi B **198**, 403 (1996).
[16] C. A. Vanderborgh, Y. K. Vohra, and A. L. Ruoff, Phys. Rev. B **40**, 12450 (1989).
[17] R. J. Nelmes and M. I. McMahon, Phys. Rev. Lett. **77**, 663 (1996).
[18] W. Utsumi, K. Funakoshi, S. Urakawa, Y. Yamakata, K. Tsuji, H. Konishi, and O. Shimomura, Rev. High Pressure Sci. Technol. **7**, 1484 (1998).
[19] K. Tsuji, K. Yaoita, M. Imai, O. Shimomura, and T. Kikegawa, Rev. Sci. Instrum. **60**, 2425 (1989).
[20] N. Funamori and K. Tsuji, Phys. Rev. B **65**, 014105 (2001).
[21] The diffraction profiles were taken at $2\theta=3°$, 4°, 5°, 6°, 8°, 10°, 12°, 15°, and 20° in the experiments at PF-AR, and at $2\theta=3°$, 4°, 5°, 6°, 8°, 11°, and 15° in the experiments at SPring-8.
[22] D. L. Decker, J. Appl. Phys. **42**, 3239 (1971).
[23] T. E. Faber and J. M. Ziman, Philos. Mag. **11**, 153 (1965).
[24] J. Mizuki, K. Kakinoki, M. Misawa, T. Fukunaga, and N. Watanabe, J. Phys.: Condens. Matter **5**, 3391 (1993).
[25] H. Krebs, J. Sutter, and H. Thurn, Z. Phys. Chem., Neue Folge **92**, 349 (1974).
[26] The positions of the peaks at ambient pressure are estimated by extrapolating the data below 6.7 GPa.
[27] K. Tsuji, Y. Katayama, Y. Morimoto, and O. Shimomura, J. Non-Cryst. Solids **205–207**, 295 (1996).
[28] Y. Morimoto, S. Kato, N. Toda, Y. Katayama, K. Tsuji, K. Yaoita, and O. Shimomura, Rev. High Pressure Sci. Technol. **7**, 245 (1998).
[29] T. Hattori, T. Kinoshita, T. Narushima, and K. Tsuji, J. Phys.: Condens. Matter **16**, S997 (2004).
[30] W. Freyland, F. Hensel, and W. Gläser, Ber. Bunsenges. Phys. Chem. **83**, 884 (1979).
[31] R. Winter, F. Hensel, T. Bodensteiner, and W. Gläser, Ber. Bunsenges. Phys. Chem. **91**, 1327 (1987).
[32] Y. Waseda, K. Shinoda, K. Sugiyama, S. Takeda, and K. Terashima, Jpn. J. Appl. Phys., Part 1 **34**, 4124 (1995).
[33] T. Itami, S. Munejiri, T. Masaki, H. Aoki, Y. Ishii, T. Kamiyama, Y. Senda, F. Shimojo, and K. Hoshino, Phys. Rev. B **67**, 064201 (2003).
[34] R. J. Nelmes and M. I. McMahon, Semicond. Semimetals **54**, 145 (1998).
[35] J. D. Barnett, R. B. Bennion, and H. T. Hall, Nature (London) **141**, 1041 (1963).
[36] The bcc-like local structure may represent the component of isotropic liquid, such as simple liquid metals, instead. It is because the $g(r)$ for both structures are very similar and they cannot be distinguished from each other.
[37] The transition pressure between the β-Sn and bcc structures in *c*-InSb is still unknown since the transition does not occur in *c*-InSb. The pressure is, however, estimated as about 11 GPa since the transition from the orthorhombic *Immm* having the structure similar to the β-Sn into the bcc structure occurs at such pressure.
[38] E. Rapoport, J. Chem. Phys. **46**, 2891 (1967).
[39] The larger entropy of the bcc structure is inferred from the phase diagram of Sn.(Ref. 35) In which the slope of phase boundary between the β-Sn and bct structures is negative. The Clasius-Clapeyron equation suggests the entropy change in the transition from the β-Sn phase into the bcc one is positive since the volume change is negative. This indicates that the bct structure has an entropy larger than that of the β-Sn structure. In the same way, the bcc structure of InSb is considered to have a larger entropy than that of the β-Sn structure.
[40] S. Hosokawa, J. Greif, F. Demmel, and W. C. Pilgrim, Chem. Phys. **292**, 253 (2003).
[41] In the diagram for *l*-GaSb, the fraction corresponding to x was written since the existence of a new high-pressure form was not known at the time the paper was written. The *l*-GaSb, however, would have the new form identical to that observed in *l*-InSb since *l*-GaSb shows almost the same pressure dependence as that of *l*-InSb. Therefore, the denser form in *l*-GaSb would be "1/2β-Sn +1/2 bcc," and the fraction in Fig. 11 of Ref. 13 should be doubled. In this case, the parameters of Rapoport model in *l*-GaSb are replaced by the following ones: $\Delta\epsilon^0=8.1\times10^{-21}$ (J/atom), $\Delta V^0=4.3$ (Å^3/atom), $\Delta S^0=4.2\times10^{-23}$ (J/K per atom), $\omega=-3.5\times10^{-21}$(J/atom), and ω/k_BT (at $T=1000$ K)$=-0.26$.
[42] E. Rapoport, J. Chem. Phys. **48**, 1433 (1968).